IN

TURBULENCE AND DIFFUSION NOTES NO 18

ON THE THICKNESS OF THE PLANETARY BOUNDARY LAYER IN DIABATIC CONDITIONS

by

D. J. CARSON

Boundary Layer Research
Met O 14
Meteorological Office HQ
Bracknell

October 1971

1. INTRODUCTION

The planetary boundary layer may be defined in general terms as the layer of the atmosphere which is significantly influenced by the underlying surface. A practical method for estimating, and indeed forecasting, the depth of the boundary layer is required, for example, in studies dealing with the dispersion of concentrations of atmospheric pollutants such as sulphur dioxide. During the daytime the vertical spread of such pollutants can be severely checked by the presence of a thermal inversion which denotes the upper limit of the well-mixed turbulent layer and in certain meteorological and geographical situtations the mixing depth is an important parameter for forecasting the concentrations of pollutants trapped beneath the inversion "lid".

A thorough investigation of many different methods currently available for estimating the thickness of the planetary boundary layer has been presented by Hanna (1969). The purpose of Hanna's paper was to compare and criticise as many of the methods as possible by applying them to the 1953 O'Neill boundary layer observations from the Great Plains Turbulence Field Program (published by Lettau and Davidson (1957)), and to attempt to recommend the most practical method.

Formulae which are known to yield good estimates of the boundary layer depth in neutral conditions are totally inadequate to deal with the diabatic conditions pertaining during the period of the O'Neill observations. Thus simple relationships between the depth, h, and u_*/f or G/f, where u_* is the surface friction velocity, G is the geostrophic wind speed at the top of the boundary layer and f is the coriolis parameter, are useful only when restricted to near neutral conditions, and so it is obviously necessary to include the effects of the departure from adiabatic conditions in any useful theoretical formulae.

The most successful correlations between theoretical and observed thicknesses were obtained by Hanna using the formulae of:

(i) Laikhtman (1961), $h = C_1 G / \left(\frac{g}{T} \cdot \frac{\Delta\theta}{\Delta z} \right)^{1/2}$, (1)

and (ii) Rossby and Montgomery (1935), $h = C_2 G \sin\alpha(0) / \left(\frac{g}{T} \cdot \frac{\Delta\theta}{\Delta z} \right)^{1/2}$, (2)

where C_1, C_2 are constants, $\Delta\theta/\Delta z$ is the mean gradient of potential temperature throughout the boundary layer, T is a mean actual temperature for the layer, g the acceleration due to gravity and $\alpha(0)$ is the angle between the limiting direction of the wind at the surface and the direction of the surface geostrophic wind. Hanna found a correlation coefficient of 0.89 between the observed depth, h_o , and the theoretical estimate of the depth, h, using formula (1), with $C_1 = 0.75$ (Laikhtman's constant was 1.36). With formula (2) Hanna obtained a correlation coefficient of 0.83 between h_o and h , with $C_2 = 1.2$ (Rossby and Montgomery had a constant of 0.38).

Although the above formulae cater reasonably well for diabatic conditions it is necessary to estimate the average vertical gradient of potential temperature over the boundary layer before the thicknesses can be evaluated. However a knowledge of the vertical temperature profile is not always available and would be difficult to predict. Other successful semi-empirical techniques discussed by Hanna meet the same problem, that a temperature sounding is required before the thickness can be estimated.

Hanna concludes that the best methods of estimating h are impractical for the ordinary observer whereas other more practical methods do not account for diabatic effects. Further, he suggests that a theory using wind speed and some measure of the stability near the surface would be desirable.

With Hanna's recommendations in mind, the present author has used the 1953 O'Neill data to explore possible correlations between the observed depth of the boundary layer and combinations of boundary layer parameters such as the surface friction velocity, u_* , and the surface Monin-Obukhov

length, L, which can be estimated from measurements made close to the ground. The derived relationships go part way to meeting the criteria laid down by Hanna and provide some encouraging correlations which should be pursued further using more recently obtained, good boundary layer observations; see, for example, "The Wangara Experiment Boundary Layer Date" by Clarke, Dyer, Brook, Reid and Troup (1971).

A feature not specifically investigated by Hanna (1969) is the evolutionary aspect of the daytime mixing depth. Ball (1960) has given a theoretical treatment for the control of the height of the inversion which frequently caps the mixing layer produced in conditions of daytime surface heating. In particular, Ball's theory predicts the rate at which the inversion will rise in dry convective conditions. A study of the growth of the daytime mixing layer at O'Neill has prompted the present author to suggest a simple relationship for estimating the depth of the layer as a function of a time integral of the sensible heat flux measured at the surface.

2. DERIVATION OF PARAMETERS FROM 1953 O'NEILL DATA

The complete details of the O'Neill Program can be found in the publication by Lettau and Davidson (1957). Here we state which parameters are required for the present study and how they are derived from the basic O'Neill observations.

(i) h_o, the observed thickness of the planetary boundary layer.

The O'Neill data include a vertical temperature sounding through the planetary boundary layer from which we can estimate h_o as the lowest level at which the vertical temperature gradient exhibits a discontinuity (Hanna, 1969). During daytime conditions when there exists a well-mixed layer near the surface beneath a more stable upper layer, h_o corresponds to the level of the base of the stable layer and denotes the 'mixing-depth'. When a stable layer exists from the surface then h_o corresponds to the top of the lowest inversion layer and denotes the region close to the ground where turbulent

mixing is most suppressed. It should be noted that this definition of h_o categorizes two physically distinct types of boundary layer, namely, the relatively deep, daytime, well-mixed layer and the relatively shallow, night-time, inversion layer.

Hanna points out that thicknesses estimated in this way from the O'Neill data are accurate only to within about 100m due to the spacing of the heights used in the temperature soundings. Having accepted Hanna's apparently objective definition for h_o it is interesting to note that the distribution of h_o adopted for the present study differs from that obtained by Hanna. Of the 95 original sets of data Hanna rejected 6 as unusable, mostly because they were obtained near sunrise or sunset when surface conditions were changing rapidly . The two distributions obtained from the remaining 89 ascents are given in Table 1, and we note that the present author adopts 50% more thicknesses of 200m than Hanna did. A certain degree of subjectivity has entered the analysis! Of the 14 cases where the two evaluations of h_o differ, 10 occur within observation periods 1, 5, 7. These periods are specifically mentioned by Hanna in connection with advection processes and indeed in part of his analysis he is obliged to correct only these three sets of temperature profiles by removing linear trends due to advection. This may well be the reason for the differences obtained in the distributions of estimated h_o.

TABLE 1. DISTRIBUTION OF OBSERVED PLANETARY BOUNDARY LAYER THICKNESS, h_o(m), AS ESTIMATED FROM THE 1953 O'NEILL DATA BY HANNA (1969) AND CARSON

h_o(m)	200	400	600	800	1000	1250	1500	1750	$\geq$ 2000	TOTAL
HANNA(1969)	14	23	18	6	4	11	2	3	8	89
CARSON	21	23	15	6	3	7	3	3	8	89

(ii) u_*, the surface friction velocity.

The surface friction velocity is estimated from the relationship,

$$u_* = \sqrt{\frac{\tau(0)}{\rho}} \quad , \qquad (3)$$

or $$u_* = k\left(z\,\partial V/\partial z\right) \quad ,$$

where $\tau(0)$ is the magnitude of the surface shearing stress, ρ is the air density close to the surface, V is the mean wind speed at height z above the surface and k is the von Karman 'constant'.

Averaged values of the required parameters are tabulated at two hour intervals within each observation period. In the second relationship the observed k was determined from measurements of averaged $\tau(0)$ and by assuming the neutral logarithmic form for the mean wind profile. Individually the values of k for the O'Neill observations vary from 0.33 to 0.45.

(iii) H, the sensible heat flux at the surface.

The values of H used are those according to Lettau's theoretical model and are tabulated, again at two hour intervals within each observation period. Values are hourly means centred at the times indicated.

From the above basic observations we construct the following boundary layer parameters:

(iv) $$h_o^* = h_o / \left(\frac{u_*}{f}\right) , \qquad (4)$$

where (u_*/f) represents the boundary layer scale height which will in neutral conditions determine the thickness of the boundary layer which observations suggest is of order 0.2 (u_*/f). Similarly we define $h^* = h/(u_*/f)$ where h is a theoretical estimate of the thickness.

(v) L, the Monin-Obukhov length for the surface layer.

$$L = \frac{-u_*^3}{k\beta\left(H/\rho c_p\right)} \qquad (5)$$

where $$\beta = g/T ,$$

T is a mean absolute temperature for the layer and c_p is the specific heat of air at constant pressure. The buoyancy parameter, β, varies little and is regarded as constant throughout the computations with a value 3.4 cm $sec^{-2} {}^oK^{-1}$

(vi) μ, a non-dimensional stability parameter.

$$\mu = \frac{ku_*}{fL} \qquad (6)$$

The parameter μ was introduced by Kazansky and Monin (1960), and has been extensively used, for example, by Monin and Zilitinkevich (1967), and by Clarke (1970) whose notation is $sk^2 (= \mu)$.

3. SEMI-EMPIRICAL FORMULAE FOR ESTIMATING THE THICKNESS OF THE BOUNDARY LAYER

If we assume that the thickness of the boundary layer is a resultant characteristic of the general turbulence field which, in turn, can be determined by certain external parameters then, following the similarity hypothesis stated by Kazansky and Monin (1960) (and discussed in papers by Monin and Zilitinkevich (1967), Clarke (1970) and Sheppard (1969)) we

we may combine the internal boundary layer parameters u_* and $H/\varrho c_p$ with the relatively constant parameters β and f to propose h^* as a function of μ only,

ie $$h^* = f(\mu) \quad , \tag{7}$$

in horizontally homogeneous, stationary conditions.

In terms of the external boundary layer parameters the equivalent statement in horizontally homogeneous, stationary conditions is

$$h/\left(\frac{G}{f}\right) = \text{function of } R_o \text{ and S only,}$$
$$= F(Ro,S), \text{ say,} \tag{8}$$

where $R_o = G/fz_o$ is the surface Rossby number,

$S = \beta \frac{\Delta\theta}{fG}$ is an external stability parameter,

z_o is the roughness length of the underlying surface and $\Delta\theta$ is the difference in potential temperature across the boundary layer.

We note that μ can be expressed as a function of Ro and S (Monin and Zilitinkevich, 1967) and that when internal parameters only are used the effects of z_o and G are included in u_*.

The formulae of equations (1) and (2) are similar to the formulation suggested in equation (8); the effect of z_o is not included explicitly in Laikhtman's formula but is implied by G and $\alpha(0)$ in the formula of Rossby and Montgomery. For the present we shall restrict our investigation to the possible form of $f(\mu)$ in relation (7) whilst recalling from our knowledge of the neutral situation ($\mu = 0$) that we should expect $f(0) \simeq 0.2$. In this way we hope to allow for the effects of stability whilst retaining the established relationship for near neutral conditions.

(i) h^* as a function of μ

The first step is to investigate the possibility of a correlation between h_o^* and μ . Linear regression techniques yield a correlation coefficient of -0.15 between the two parameters when all stability categories are included in the analysis, -0.04 when stable ($\mu > 0$)

cases only are included and -0.36 when unstable ($\mu < 0$) cases only are included.

The lack of correlation between the variables h_o^* and μ is at first sight very discouraging and suggests that the formulation proposed in equation (7) is not a viable prospect.

One of the main assumptions which allowed us to state equation (7) is that conditions are stationary over a time which includes the observation period. Sheppard (1969) has pointed out that the term 'stationary' can strictly only be applied if conditions have remained effectively steady over a period of a few hours. Non-stationarity will arise naturally over a land surface due to the relatively rapid diurnal variations of the radiation flux and for this reason alone the conditions in the boundary layer during the O'Neill observational periods must be classed as non-stationary. It is perhaps not unreasonable then that there should be no significant correlation between h_o^* and μ, since the observed boundary layer thickness h_o at time t is not the equilibrium thickness resulting from stationary conditions controlled by parameters u_*/f and μ whose mean values we have estimated over a period centred on time, t.

Variations in the external parameters which govern the state of the planetary boundary layer will be reflected in interrelated changes in the distributions of wind, temperature and turbulence within the layer. In particular a variation in the radiation flux at the surface with subsequent stationary conditions will cause the wind, temperature and tubulent exchange fields to vary interdependently and continue to vary until profiles have been established which meet the conditions for thermal and dynamical equilibrium within the boundary layer corresponding to the new values of the external parameters. A detailed

discussion of the external factors which determine the structure of the planetary boundary layer has been presented by Laikhtman (1961).

A major consequence of a variation in the surface heating is the resulting change in the temperature profile throughout the boundary layer which is reflected in changes in the lapse rates between levels and the thickness, h_o, estimated from the gradient discontinuities.

In non-stationary conditions the wind, temperature and turbulent exchange fields are continuously re-adjusting to meet the variations in the determining external parameters. If the main cause for the non-stationarity is the diurnal variation in the radiation flux, then we should expect that although the boundary layer is in a state of constant re-adjustment, the reforming of the profile gradients is virtually a quasi-continuous process, also with a diurnal mode, and that an instantaneous profile will, as a whole, be characteristic of the mechanical and thermal turbulence fields averaged over a somewhat earlier period. There is a lag, then, between the effect of an external change being sensed at the surface and that change being reflected in the overall boundary layer profiles. However, if the external variations are occurring smoothly and not too rapidly, the profiles will adjust continuously to the new conditions and we might hope then to find a significant correlation between the observed "instantaneous" boundary layer thicknes, h_o, and some combination of the average mechanical turbulence intensity and the thermal stratification parameter averaged over a slightly earlier period.

For non-stationary conditions characterized by a continuous but not too rapid variation in an external parameter the above argument leads us to propose

$$h^*(t-\delta t) = \text{function of } \mu(t-\delta t),$$
$$= f(\mu(t-\delta t)), \text{ say,} \qquad (9)$$

where

$$h^*(t-\delta t) = h(t) \Big/ \left(\frac{u_*}{f}(t-\delta t)\right) , \qquad (10)$$

and, similarly,

$$h_o^*(t-\delta t) = h_o(t) \Big/ \left(\frac{u_*}{f}(t-\delta t)\right) ,$$

δt is a time interval to be defined, and for any quantity, Q, other than h^*, h_o^*, Q(t) denotes the value of Q estimated at time t or, in the case of time-averaged quantities, the value of Q measured over a period of time centred on time t.

We note that this formulation is proposed for external variations such as the diurnal variation of radiation but it does not take into account non-stationary conditions dominated by processes such as advection. Problems will no doubt also arise in the neighbourhood of sunrise and sunset when surface conditions are changing rapidly and the surface boundary layer is changing in nature as a result of the change in sign of the surface sensible heat flux. The adopted time interval δt obviously has bounds outside of which any attempt at correlation would prove futile. In this study we shall correlate ho(t) with boundary layer parameters estimated for the period centred on the time of the previous ascent. This implies δt of the order of two hours which is probably close to the limiting value.

(ii) $h^*(t-\delta t)$ as a function of $\mu(t-\delta t)$.

From the 95 sets of data obtained at O'Neill, 74 pairs $(\mu(t-\delta t), h_o^*(t-\delta t))$ are formed and are plotted in Figure 1. With all the data included in the analysis the best fit linear regression line for $ho^*(t-\delta t)$ regressed on $\mu(t-\delta t)$ gives us an estimate for $h^*(t-\delta t)$,

$$h^*(t-\delta t) = f(\mu(t-\delta t))$$
$$\simeq 0.15 - 0.0023\,\mu(t-\delta t), \qquad (11)$$

where the correlation coefficient between the two regression variables is -0.69 and the variance about the regression line yields a standard error of estimate for the $ho^*(t-\delta t)$ of 0.08 (ie r = -0.69, $s_{ho}^* = \sigma_{h_o^*}\sqrt{(1-r^2)}$

= 0.08, where r is the correlation coefficient, $\sigma_{h_o^*}$ is the standard deviation of $h_o^*(t - \delta t)$ for the sample and $s_{h_o^*}$ is the standard error of estimate when estimating $h_o^*(t - \delta t)$ from the regression line of equation (11)).

Although the scatter is very high (52% of the variance is not accounted for by the regression) the correlation is highly significant, with the level of significance less than 0.1%, and in this sense the results are very encouraging. In particular, equation (11) implies

$$f(0) \simeq 0.15 \qquad (12)$$

ie $$h(t) \simeq 0.15 \frac{u_*}{f} (t - \delta t)$$ in neutral conditions,

which is in close agreement with other observational evidence.

Linear regression techniques applied to only the unstable cases yield a higher correlation coefficient of -0.77 which is again highly significant although the regression line implies,

$$h^*(t - \delta t) \simeq 0.067 - 0.0038\, \mu(t - \delta t), \quad (\mu < 0), \qquad (13)$$

which does not suggest as good a value for $f(0)$ as equation (11).

The distribution of points in Figure 1 suggests a non-linear best fit curve rather than a linear one and the second order polynomial regression line which best fits the sample implies,

$$h^*(t - \delta t) = f(\mu(t - \delta t))$$
$$\simeq 0.13 - (21 \times 10^{-5})\, \mu(t - \delta t) + (315 \times 10^{-7})\, \mu^2(t - \delta t), \qquad (14)$$

which gives an index of correlation between the sample variables, $\mu(t - \delta t)$ and $h_o^*(t - \delta t)$, of 0.78 (ie 40% of the variance is not accounted for by the regression) and a standard error of estimate 0.07.

The function of equation (14) is plotted in Figure 1 and we note that it has a minimum value of approximately 0.13 at $\mu(t - \delta t) \simeq 3.3$. The arguments leading to an attempted relationship between the depth of the boundary layer and the general turbulence parameters are not so obviously

meaningful for the shallow stable boundary layer, where mechanical turbulence is suppressed, as they are for the evolving, generally deeper, well-mixed turbulent layers corresponding to $\mu \leq 0$.

If we accept the relation (14) as giving our best estimate of $h^*(t-\delta t)$ based on the measurement of $\mu(t-\delta t)$ then we can rewrite it to express h(t) as a function of $\frac{u_*}{f}(t-\delta t)$ and $L(t-\delta t)$, so

$$h(t) \simeq \left[0.13 \frac{u_*}{f} - (21 \times 10^{-5}) \left(\frac{u_*}{f}\right)^2 \cdot \frac{k}{L} + (315 \times 10^{-7}) \left(\frac{u_*}{f}\right)^3 \cdot \left(\frac{k}{L}\right)^2 \right]_{t-\delta t} \quad (15)$$

In Figure 2 we see the contours for $L(t-\delta t)$ = constant in the h(t), $\frac{u_*}{f}(t-\delta t)$ plane, derived from equation (15). On the unstable side the regression analysis which led to equation (15) was only applied to data with $L \lesssim -14$ and so strictly the contours of L should be limited to this range. For a given u_* there exists an $L_{crit}(u_*)$ on the stable side such that h(t) has a minimum value at that L for the given u_*. Thus equation (15) implies that h(t) increases for $L < L_{crit}(u_*)$ on the stable side; however the mechanisms causing the depth of an inversion layer to increase would have to be studied more thoroughly to determine whether or not this increase in depth with increase in stability beyond $L_{crit}(u_*)$ is valid. The contours are illustrated only for the neutral and unstable cases.

We note also that the range of u_* observed at O'Neill varies systematically with the stability, however the observed range of u_* does not simply increase as stability decreases. The variation of u_* with L as measured at O'Neill is shown in Figure 3 and the suggestion is that the relationship is non-linear with the highest values of u_* occurring in the slightly unstable and near-neutral categories, indicating that the highest winds are generally found in near-neutral conditions. For given values of L typical values of u_* are obtained from the eye-fit curve in Figure 3 and h(t) are estimated from

equation (15) to produce the broken line in Figure 2 which indicates the typical order of h(t) one would expect to obtain given $\frac{u_*}{f}(t-\delta t)$ and $L(t-\delta t)$ where δt is of the order of two hours, for a site with roughness characteristic of O'Neill.

Figure 4 shows the correlation between $h_o(t)$, the thickness observed from the vertical temperature profiles, and h(t) obtained from equation (15). The linear regression of ho(t) on h(t), where both are in metres, is

$$ho(t) \simeq 6 + 0.97\, h(t)$$
$$\simeq h(t) \quad ,$$

where the correlation coefficient is 0.81 (ie 34% of the variance is not accounted for by the regression) and the standard error of estimate for ho(t) is approximately 330m. Although the standard error is rather higher than we would like the correlation between ho(t) and h(t) is highly significant and the correlation coefficient is of the same order as that obtained using the acceptable formula (2) due to Rossby and Montgomery (1935). A formulation of the type

$$h(t) = \left[A \frac{u_*}{f} + B \left(\frac{u_*}{f}\right)^2 \cdot \frac{k}{L} + C \left(\frac{u_*}{f}\right)^3 \cdot \left(\frac{k}{L}\right)^2 \right]_{t-\delta t} \qquad (16)$$

used in equation (15), where A, B and C are dimensionless constants to be determined by regression techniques, and δt is a time interval of order one to two hours would appear to yield encouraging results when used to estimate the depth of the boundary layer.

(iii) $h^*(t-\delta t)$ as a function of $L(t-\delta t)$

The relative success of the formulation of equation (9) encourages us to investigate similar formulations involving u_*/f and L. One such is the suggestion that we might express $h^*(t-\delta t)$ as a function of stability only where $L^{-1}(t-\delta t)$ is used as the stability parameter, ie

$$h^*(t-\delta t) = \text{function of } L^{-1}(t-\delta t) \text{ only,}$$
$$= g\left(L^{-1}(t-\delta t)\right), \text{ say.} \qquad (17)$$

Note that in this case the L.H.S. is non-dimensional whereas the variable L^{-1} has dimensions $[\text{length}]^{-1}$. It will be assumed that

L is measured in metres whenever a functional form for $g(L^{-1}(t-\delta t))$ is given.

Following the pattern of the previous section we obtain estimates of $h^*(t-\delta t)$ by regressing $h_o^*(t-\delta t)$ on $L^{-1}(t-\delta t)$. Linear regression fitting gives

$$h^*(t-\delta t) = g(L^{-1}(t-\delta t)) \simeq 0.16 - 2.93\, L^{-1}(t-\delta t), \tag{18}$$

with correlation coefficient 0.64 when all 74 cases are considered, and

$$h^*(t-\delta t) = g(L^{-1}(t-\delta t)) \simeq 0.09 - 5.94\, L^{-1}(t-\delta t), \tag{19}$$

with correlation coefficient -0.79 when only the unstable cases are considered. Second order polynomial regression gives

$$h^*(t-\delta t) = g(L^{-1}(t-\delta t)) \simeq 0.14 - 1.62\, L^{-1}(t-\delta t) + 46.31\, L^{-2}(t-\delta t), \tag{20}$$

with an index of correlation 0.75 (44% of the variance is not accounted for by the regression), a standard error of estimate 0.08 and a minimum turning point on the stable side at $L^{-1} = 0.0175\ m^{-1}$ ($L \simeq 57m$). Figure 5 gives the distribution of the sample pairs $(L^{-1}(t-\delta t), h_o^*(t-\delta t))$ and the function $g(L^{-1}(t-\delta t))$ as estimated by the regression line of equation (20). If we accept equation (20) as giving the best estimate of $h^*(t-\delta t)$ from regression then we can write

$$h(t) \simeq \left[(0.14 - 1.62\, L^{-1} + 46.31\, L^{-2}) \frac{u_*}{f} \right]_{t-\delta t} \tag{21}$$

for our best estimate of the boundary layer thickness based on the measurement of $\frac{u_*}{f}(t-\delta t)$ and $L^{-1}(t-\delta t)$. We note that this latest expression for estimating $h(t)$ is linear in $\frac{u_*}{f}(t-\delta t)$ for an explicit value of $L(t-\delta t)$ whereas the relation in equation (15) is cubic in $\frac{u_*}{f}(t-\delta t)$ for a given $L(t-\delta t)$. Figure 6 gives the contours for $L(t-\delta t)$ = constant in the $h(t)$, $\frac{u_*}{f}(t-\delta t)$ plane, based on equation (21). Recall that on the unstable side the contours should strictly be limited to the sample range, $L \lesssim -14$ and that on the stable side the regression

equation (21) implies that h(t) will begin to increase for $L \lesssim 57$. Also indicated in Figure 6 is the order of h(t) one would expect to obtain given $\frac{u_*}{f}(t-\delta t)$ and $L(t-\delta t)$ for a site with roughness characteristic of O'Neill, the values being based on the u_*, L^{-1} relationship suggested in Figure 3 and h(t) evaluated from equation (21). Values of h(t) from equation (21) are compared in Table 2 with those obtained from equation (15) under the same set of typical conditions and we note the close agreement obtained.

TABLE 2. VALUES OF h(t) ESTIMATED FROM EQUATIONS (15) AND (21) FOR TYPICAL VALUES OF THE PARAMETERS $u_*(t-\delta t)$ (m sec^{-1}) and $L(t-\delta t)$(m)

$L(t-\delta t)$ (m)	$u_*(t-\delta t)$ (m sec^{-1})	h(t)(m) EQN.(15)	h(t)(m) EQN.(21)
60	0.225	301	283
75	0.26	345	330
$\pm\infty$	0.475	617	665
-100	0.62	957	997
- 50	0.525	1020	1002
- 30	0.43	1046	1049
- 20	0.385	1281	1297
- 15	0.365	1650	1666
- 12	0.36	2177	2137

In Figure 7 the observed thickness ho(t) is plotted against h(t) obtained from equation (21). The best fit linear regression line of ho(t) on h(t)is

$$ho(t) = -65 + 1.1\, h(t) \simeq h(t)$$

the correlation coefficient is 0.81 (i.e. 34% of the variance is not accounted for by the regression) and the standard error of estimate for

$h_o(t)$ is again approximately 330m. It would appear, from the present sample, that a formulation of the type

$$h(t) = \left[(D - EL^{-1} + FL^{-2}) \frac{u_*}{f} \right]_{t-\delta t} \qquad (22)$$

where D, E and F are dimensional constants to be determined from regression analysis, and δt is a time interval of order one to two hours, provides as good an estimate of the boundary layer thickness as the formulation of equation (16).

Extension of these ideas to the more unstable cases with much deeper boundary layers might help to determine which, if either, of the above formulations is the more useful.

4. EVOLUTIONARY ASPECTS OF THE BOUNDARY LAYER THICKNESS

One of the main problems which arises when one is dealing with diabatic conditions is that they are characteristically non-stationary situtations. This is undoubtedly one of the biggest reasons for the marked degree of scatter about the regression lines of the previous section and this scatter should be borne in mind if it is decided to use any of the above formulae to predict a thickness for the boundary layer on any particular occasion.

It has already been stated that the depth of the boundary layer is closely correlated to the diurnal variation in radiation flux recorded at the underlying surface. It is of interest then to compare the diurnal variations in the thickness of the boundary layer and the sensible heat flux entering or leaving the layer through the underlying surface. For this reason the heat flux values from Lettau's theoretical model, recorded at two hour intervals within each observation period, are averaged and the mean values, $\langle H(t) \rangle$, and standard errors of the means (standard deviation of sample/(number in sample)$^{1/2}$) are plotted in Figure 8 to give an average diurnal pattern of sensible heat flux as observed during the seven observational periods from

13 August - 8 September 1953 at O'Neill. The time of day is expressed in Mean Solar Time (MST), where MST is the local standard time (CST) minus 34 mins. Throughout the observational period, Sunrise occurred at approximately 0530 MST, apparent noon at 1200 MST and sunset at approximately 1900 MST. The smooth average curve indicates that the heat flux changes sign within one hour after sunrise, reaches a maximum value close to apparent noon, and changes sign once again about 1½ hours before sunset.

The ascents at O'Neill were classified by means of a coefficient which approximates to a height derivative of a Richardson number from the surface to 16m and can be considered as a convenient bulk parameter which measures the overall convective stability of the lowest 16m. The distribution of the stability classes measured in this way during the Great Plains Turbulence Field Program is given in Lettau and Davidson (1957).

In the period 1900-0700 MST the stability classes refer to inversions with the exception of four neutral classifications for the period around 0600 MST. All observed boundary layer depths determined during this interval will be classed in the present study as pertaining to the stable type boundary layer.

In the period 0900-1700 MST the stability classes refer to lapses with the exception of four neutral classifications in the period around 1600 MST. All observed boundary layer depths determined during this interval will be attributed to the unstable type boundary layer.

The period centred on 0800 MST is a transitional period when the night-time inversion is being eroded by the turbulence and heating close to the ground and so, although the lowest 16m are always indicating lapse or neutral categories, the vertical profiles on the broader scale are occasionally indicating the top of the inversion as the first discontinuity in temperature gradient but at other times are already indicating the development of the daytime layer. Similarly, the period centred on 1800 MST is a transitional period. The stability classes for the surface layer indicate that the night-time inversion is already establishing itself by this period, however again

the large scale profiles may still be indicating the top of the daytime mixing depth as the first discontinuity in temperature gradient. This will be taken into account when the thicknesses are averaged.

We average the observed heights for all the bi-hourly runs within the observational periods at O'Neill and plot the mean depths of the boundary layer, $\langle h_o(t) \rangle$, with their standard errors against time of day, in Figure 8. Note that the suggested mean curve for the depth of the boundary layer is discontinuous in the neighbourhoods of sunrise and sunset. In general the hours between sunset and sunrise refer to the depth of the stable boundary layer whereas between sunrise and sunset (or more strictly when the sensible heat flux measured at the surface is positive) the interest is in the evolution of the daytime mixing depth.

Two points should be noted:

(i) When the mixing depth was observed to be $>$ 2000m (the upper limit of the temperature soundings) it was taken as 2000m for averaging purposes. Therefore the mean values forthe unstable layers between 1400-1800 MST are probably on the low side.

(ii) The mean value for the mixing depth at 1600 MST is affected quite severely by the two low heights observed during the fifth observation period when there was marked advection. With these two values omitted the mean value is of the order of 1700m and this value has been adopted to determine the shape of the mean boundary layer depth curve between 1400-1900 MST.

Obviously there is a degree of subjectivity in the curve drawn in Figure 8.

Comparison of the mean diurnal curves for $\langle ho(t) \rangle$ and $\langle H(t) \rangle$ in Figure 8 suggests a strong correlation between the sensible heat flux and the observed depth during daytime. In Figure 9 we have plotted the mean boundary layer thickness at two hour intervals against the mean sensible

heat flux averaged during a period two hours before the depths were observed. The resulting curve supports the use in earlier sections of correlations between observed boundary layer thicknesses and characteristics of the turbulence fields measured at an earlier period.

There is little significant evolutionary trend in the depth of the night-time stable layer in which buoyancy and viscous forces combine to suppress any mechanically generated turbulent motions. However, the depth of the daytime mixing layer is closely correlated to the diurnal pattern of the surface heating. The growth of the mixing depth is shown to continue so long as the surface heat flux continues to increase in the positive sense. The suggested evolution of the boundary layer depth when the heat flux remains positive but begins to decay is more subjective, but the indications are that its evolution will continue more slowly and, no doubt, the interaction between stable and unstable air, through the temperature gradient discontinuity which caps the deep mixing layer, will play a more dominant role in determining the height of the upper inversion than the turbulence generated by the declining heating effects at the surface. We restrict this investigation to looking at the unstable layer which is capped by a fairly sharp inversion which has itself evolved as a result of the turbulent mixing in the layers below. What happens to the upper inversion when a lower inversion is established from the surface is another question which will not be considered here.

The rate at which an inversion will rise in dry convective conditions has been studied and predicted by Ball (1960) who considered the more complex effects of interaction between the processes of surface heating, mass transfer downwards from the upper stable layer into the convective layer by entrainment, subsidence and advection. An example, typical of daytime summer conditions with clear weather and a dry surface allows Ball to predict an upward movement of the inversion height of about 150m hr^{-1}. This is before

processes such as subsidence and advection have been invoked to counter the effects of surface heating and entrainment of air from above. In comparison Figure 9 suggests that for the period, 13 August - 8 September 1953, the mean upward movement of the inversion between 0800-1400 MST was approximately 250m hr^{-1}. Note also that for the daytime layer Figure 9 implies two values of $\langle ho(t) \rangle$ for each value of $\langle H(t-\delta t) \rangle$, one ordinate corresponding to increasing $\langle H(t-\delta t) \rangle$ and the other corresponding to decreasing $\langle H(t-\delta t) \rangle$.

Figures 8 and 9 suggest the following simplified formulation for the mean depth of a daytime mixing layer in conditions of strong surface heating with a diurnal mode. It is proposed that the rate of change of the mean depth $\langle h(t) \rangle$ with time is proportional to the mean amount of sensible heat being transferred up from the surface and inversely proportional to the depth through which this heat flux is distributed, namely $\langle h(t) \rangle$. Therefore we write

$$\frac{\partial}{\partial t} \langle h(t) \rangle \propto \frac{\langle H(t) \rangle}{\langle h(t) \rangle} , \qquad (23)$$

which when integrated yields

$$\langle h(t_1) \rangle^2 - \langle h(t_o) \rangle^2 \propto \int_{t_o}^{t_1} \langle H(\tau) \rangle \, d\tau .$$

If we choose t_o (=0) when $\langle h(t) \rangle = 0$, i.e. time t_o coincides with the emergence of the unstable layer (approximately 0600 MST for the mean observed depth, $\langle h_o(t) \rangle$, in our analysis), then at any subsequent time, t, the mean depth of the unstable layer is given by,

$$\langle h(t) \rangle \propto \left[\int_o^t \langle H(\tau) \rangle \, d\tau \right]^{1/2} . \qquad (24)$$

This hypothesis is tested by evaluating the R.H.S. of equation (24) graphically from the curve for $\langle H(t) \rangle$ in Figure 8 and plotting the values obtained against $\langle ho(t) \rangle$, also evaluated for given t from Figure 8. By regressing $\langle ho(t) \rangle$ on the square root of the integral in

equation (24) for hourly values between 0700 and 1800 MST we obtain the linear regression fit.

$$\langle h_o(t) \rangle = 130 \left[\int_o^t \langle H(\tau) \rangle \, d\tau \right]^{1/2} - 252, \qquad (25)$$

where $\langle h_o(t) \rangle$ is in metres, t is in hours and $\langle H(t) \rangle$ is in mwatt cm^{-2}. The correlation coefficient between the two variables is 0.983 (only about 3.5% of the variance is not accounted for by the regression) obviously highly significant, and the standard error of estimate of $\langle h_o(t) \rangle$ is 119m.

Recalling the arguments that a change in the surface heat flux requires time to make its impact on the evolution of h(t), we try reformulating (23) such that,

$$\frac{\partial}{\partial t} \langle h(t) \rangle \propto \frac{\langle H(t - \delta t) \rangle}{\langle h(t) \rangle},$$

which implies $$\langle h(t) \rangle \propto \left[\int_o^{t-\delta t} \langle H(\tau) \rangle \, d\tau \right]^{1/2}, \qquad (26)$$

where we have assumed, for the purposes of estimating the depth of the unstable layer, that $\langle H(t) \rangle \cong 0$ for $t < 0$.

With $\delta t = 1$ hour, the correlation coefficient between $\langle h_o(t) \rangle$ and the R.H.S. of (26) is 0.987 (only about 2.5% of the variance is not accounted for by the regression) and the standard error of estimate of $\langle h_o(t) \rangle$ is 95m using the linear regression line

$$\langle h_o(t) \rangle = 121 \left[\int_o^{t-1} \langle H(\tau) \rangle \, d\tau \right]^{\frac{1}{2}} - 4$$

$$\simeq 121 \left[\int_o^{t-1} \langle H(\tau) \rangle \, d\tau \right]^{\frac{1}{2}}, \qquad (27)$$

where again $\langle h_o(t) \rangle$ is in metres, t is in hours and $\langle H(t) \rangle$ is in mwatt cm^{-2}.

For $\delta t = 2$ hours the correlation coefficient between the two variables dropped to 0.975 with only ten pairs in the regression sample, however equation (27) suggests again that there would appear to be a case for correlating the depths with surface parameters measured at an earlier stage.

We define

$$\langle I \rangle_{\delta t} = \left[\int_{o}^{t-\delta t} \langle H(\tau) \rangle \, d\tau \right]^{\frac{1}{2}} , \qquad (28)$$

and $\langle h(t) \rangle_{\delta t}$ as the value of the mean boundary layer thickness, $\langle h(t) \rangle$, estimated from the regression relation involving $\langle I \rangle_{\delta t}$.

Similarly we define

$$I_{\delta t} = \left[\int_{o}^{t-\delta t} H(\tau) \, d\tau \right]^{\frac{1}{2}} , \qquad (29)$$

and $h(t)_{\delta t}$ as the value of $h(t)$ estimated from a regression relation involving $I_{\delta t}$. Note that such definitions are required if any attempt is made to use regression equations of the form

$$h(t) \simeq h(t)_{\delta t} = a(\delta t) \, I_{\delta t} + b(\delta t) , \qquad (30)$$

where $a(\delta t)$ and $b(\delta t)$ are dimensional regression coefficients, to estimate a specific value of the boundary layer thickness on a particular occasion as distinct from using the averaged values $\langle h_o(t) \rangle$, $\langle H(t) \rangle$ presented in Figures 8 and 9.

Figures 10 and 11 illustrate the distributions of the pairs ($\langle I \rangle_o$, $\langle h_o(t) \rangle$) and the pairs ($\langle I \rangle_1$, $\langle h_o(t) \rangle$) along with the linear regression lines of equations (25) and (27) which respectively give $\langle h(t) \rangle_o$ and $\langle h(t) \rangle_1$, both of which provide estimates of $\langle h(t) \rangle$. The suggestion in Figure 10 is that a best eye-fit curve would have the non-linear form suggested by the curve E_o, however the need for a non-linear fit is less apparent in Figure 11. The estimates $\langle h(t) \rangle_o$ and $\langle h(t) \rangle_1$ can also be compared with the observed $\langle h_o(t) \rangle$ in Figures 9, 12 and 13.

The success of the above relations derived from averaged values of heat fluxes and depths encourages us to try fitting regression lines of the form given in (30) to provide estimates of $h(t)$ on any particular occasion. Using only the data between 0700 and 1800 MST from the observation periods 1, 2, 3,

6, 7 to correlate $h_o(t)$ with I_o and I_1 we obtain the regression relations

$$h(t) \simeq h(t)_o = 13 + 105.5\, I_o \simeq 106\, I_o, \quad (31)$$

and $$h(t) \simeq h(t)_1 = 235 + 97\, I_1 , \quad (32)$$

where the correlation coefficient between $h_o(t)$ and I_o is 0.80 and between $h_o(t)$ and I_1 is 0.77 and in both cases the standard error of estimate of $h_o(t)$ is approximately 400m. In Figures 12 and 13 $h(t)_o$ and $h(t)_1$ have been estimated and plotted against hourly estimates of $h_o(t)$, obtained by graphical interpolation of the given two hourly values. The evolution of the parameters $h_o(t)$, $h(t)_o$ and $h(t)_1$ can be followed during any particular period by tracing the values from bottom left to top right across the graphs. The first points in Figure 12 correspond to 0700 MST and in Figure 13 to 0800 MST, thereafter points correspond to hourly intervals. In general the estimates of $h(t)_o$, $h(t)_1$ indicate fairly adequately the growth of the daytime mixing layer from shortly after sunrise until mid-afternoon. In fact most of the earlier points in Figures 12, 13 lie close to or within 1/2 - standard error of the lines $h_o(t) = h(t)_{St}$ and in this respect the high standard error of 400m is rather misleading. Period 7 gives a particularly poor fit but this was one of the periods in which advection was evident at O'Neill. Period 5 has been omitted for this reason.

5. DISCUSSION

In his paper on the thickness of the planetary boundary layer, Hanna (1969) concluded that, in order to provide an observer with a practical method for estimating the depth of the boundary layer in diabatic conditions, it is necessary to construct a formula which requires only measurements made near the ground. The first part of the present paper is an attempt to provide such a formula by investigating correlations between the depth of the boundary layer, as observed during the 1953 O'Neill experiments, and combinations of the surface layer parameters u_*, L.

In order to apply formulations of the type suggested, the observer requires a method for evaluating the parameters u_* and L based on reasonably simple ground based measurements. In the event of no more information being available, an estimate of u_* can be obtained from a knowledge of the site's roughness and a wind speed recorded within a few metres of the surface, where the conventional logarithmic wind profile might be expected to approximate to the true profile. A crude estimate of L could be deduced from general observations such as cloud cover, wind speed, time of day, month of year, etc. A better method requires only the measurement of the mean wind speed and the air temperature at two suitably spaced levels within the surface layer, where the vertical fluxes are considered to be virtually independent of height. In order to employ the method we require a knowledge of the following relationships.

The gradient Richardson number at height z is expressed in terms of the gradients of wind speed and potential temperature measured at the height,

$$Ri(z) = \frac{g}{\theta} \cdot \frac{\partial\theta/\partial z}{(\partial V/\partial z)^2} \quad , \qquad (33)$$

$$= \frac{z}{L} \cdot \left(\frac{\varphi_H(z/L)}{\varphi_m^2(z/L)} \right) \quad , \qquad (34)$$

where φ_H , φ_m are functions of z/L only and are related to the wind speed and temperature gradients and the turbulent fluxes through

$$\frac{\partial V}{\partial z} = \frac{u_*}{kz} \varphi_m \left(\frac{z}{L}\right) \quad , \qquad (35)$$

$$\frac{\partial \theta}{\partial z} = \frac{T_*}{kz} \varphi_H \left(\frac{z}{L}\right) \quad ,$$

and u_*, T_* are related through the sensible heat flux so,

$$u_* T_* = \frac{-H}{\rho c_p} \quad .$$

The functions $\varphi_m(z/L)$, $\varphi_H(z/L)$ have been evaluated by several authors and, at the present time, the work of Dyer and Hicks (1970) is recommended for the unstable cases ($L < 0$) and the work of Webb (1970) is recommended for the stable regime ($L > 0$). It should however be noted that the forms for these functions are not universally agreed upon and that no

acceptable relationships exist for cases of extreme instability ($^{z}/_{L} < -1$) and cases of extreme stability ($^{z}/_{L} \geq 6$).

It can be seen from the above relations that measurements of wind and temperature at two levels provide an estimate of the Richardson number from equation (33), which in turn implies a value of L, using (34) and the suggested forms for φ_M and φ_H. Finally, equation (35) yields u_*. The above method has been outlined in order to vindicate the use of the parameters u_* and L in a "practical" formula by indicating the relative ease with which they can be estimated from simple ground based measurements.

The investigation itself produced two formulae, equations (15) and (21), which yield values for h(t) which correlate fairly successfully with the observed values, $h_o(t)$, the correlation coefficient being approximately 0.81 in both cases. The standard error in estimating individual thicknesses is uncomfortably high, however Figures 2 and 6 should indicate the basic nature of the relationship between h, u_* and L. Two points in particular arise from the results:

(i) The formulae take account of diabatic effects with some degree of success whilst retaining the previously established form for the thickness of the boundary layer in neutral, steady state, barotropic conditions, namely, $h \propto {}^{u_*}/_{f}$, where the constant of proportionality lies in the range 0.1-0.2. One obvious drawback of the formulae of Laikhtman (1961) and Rossby and Montgomery (1935), encountered by Hanna (1969), is that they cannot be used in near adiabatic conditions when the mean potential temperature gradient through the layer is close to zero. Our new formulae do not meet with this difficulty.

(ii) Our investigation has led us to associate the depth of the boundary layer at time t with values of the parameters u_*, L at some earlier time, $t - \delta t$, where δt is of the order of 1-2 hours. A reason for this type of correlation has been put forward but should nontheless be tested on other suitable data which becomes available.

Certainly the validity and usefulness of formulae of the type suggested in equations (16) and (22) should be tried and tested on independent data.

The second part of the investigation attempts to treat the depth of the boundary layer from an evolutionary aspect. It is felt that in certain circumstances the history of the development of the daytime layer is more important in determining its depth than specific measurements made in the wind, temperature and turbulence fields at the time of interest. This point is amplified in Figure 9 where we note that the relationship between the daytime thickness and the sensible heat flux suggests a hysteresis effect in the sense that the value of $\langle h_o(t) \rangle$ for a particular $\langle H(t-\delta t) \rangle$ depends upon whether $\langle H(t-\delta t) \rangle$ is increasing or decreasing with time.

The very high correlations obtained between $\langle h_o(t) \rangle$ and $\langle I \rangle_{\delta t}$ for $\delta t = 0, 1$ give weight to our hypothesis that the history of the mixing layer is important for the cases we have studied and also indicates that during the O'Neill observation periods (excepting those in which advection was notably present) the dominating mechanism governing the development of the unstable boundary layer is the thermal turbulence generated as a result of the strong incoming radiation and that mechanically generated turbulence is of secondary importance.

Simple relations of the form given in equation (30), suggested by equations (25) and (27) and illustrated in Figures 12, 13, neglect all processes other than direct surface heating but the evolutionary trend in h(t) obtained from integrated sensible heat values is ideally suited for incorporating into numerical models which wish to simulate diurnal variations in the boundary layer under strong heating conditions. The encouraging results obtained for the mixing layer from this type of approach unfortunately throw some doubt on the validity of using the type of formulation suggested in the first part when dealing with non-steady situations.

REFERENCES

1. Ball, F. K. 1960 'Control of inversion height by surface heating' Quart. J. R. Met. Soc., 86, pp.483-494.

2. Clarke, R. H. 1970 'Observational studies in the atmospheric boundary layer', Quart. J. R. Met. Soc., 96, pp.91-114.

3. Clarke, R.H., Dyer., A.J., Brook, R.R., Reid, D.G. and Troup, A.J. 'The Wangara Experiment: Boundary Layer Data', Division of Met. Physics Tech. Paper No.19, CSIRO, Australia 1971.

4. Dyer, A.J. and Hicks, B.B. 1970 'Flux-gradient relationships in the constant flux layer', Quart. J. R. Met. Soc., 96, pp.715-721.

5. Hanna, Steven, R., 1969 'The Thickness of the Planetary Boundary Layer', Atmospheric Environment, 3, pp.519-536.

6. Kazansky, A. B. and Monin, A. S. 1960 'A Turbulent Regime above the Ground Atmospheric Layer', Izv. Acad. Sci., U.S.S.R. Geoph. Ser. No.1, pp.110-112, English translation, A.G.U.

7. Laikhtman, D.L. 1961 'Physics of the Boundary Layer of the Atmosphere', Leningrad (Gidro-meteoizdat), 8°, pp.253.

8. Lettau, H.H. and Davidson, B. 1957 'Exploring the Atmosphere's First Mile', Pergamon Press, London-New York-Paris, 2 vols.

9. Monin, A.S. and Zilitinkevich, S.S. 1967 'The planetary boundary layer and large-scale atmospheric dynamics', The Global Atmospheric Research Programme, Report of the Study Conference held at Stockholm, 28 June-11 July 1967. I.C.S.U./I.U.G.G. Committee on Atmospheric Sciences and COSPAR.

10. Rossby, C.G. and Montgomery, R.B. 1935 'The layer of frictional influence in wind and ocean currents', Pap. phys. Oceanog. Met. 3, (3), 101 pp.

11. Sheppard, P.A. 1969. 'The atmospheric boundary layer in relation to large-scale dynamics', pp.91-112. The Global circulation of the Atmosphere, R. Met. Soc.

12. Webb, E.K. 1970 'Profile relationships: the log-linear range, and extension to strong stability', Quart. J.R. Met. Soc., 96, pp.67-90.

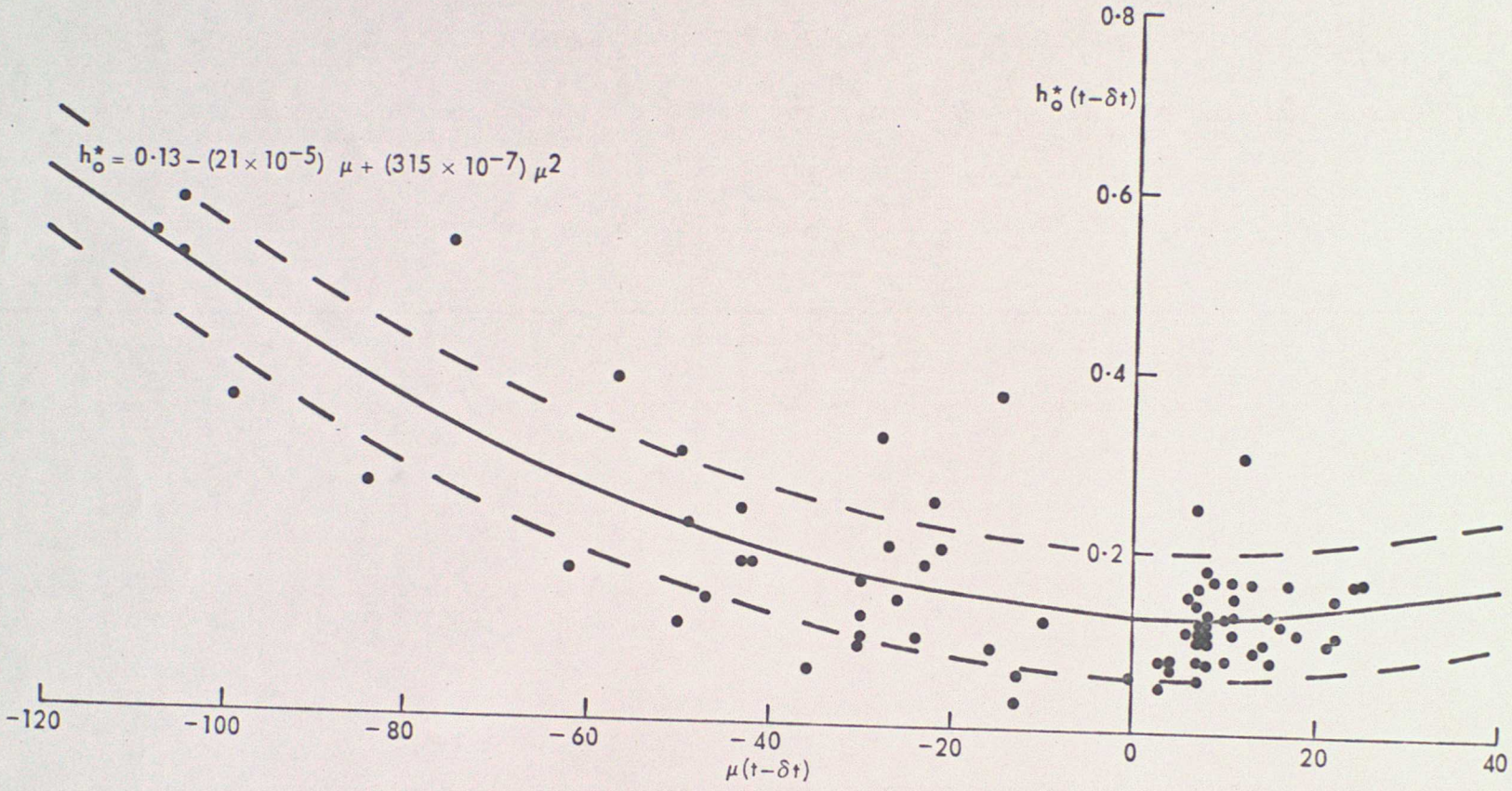

Figure 1. $h_o^*(t-\delta t)$ as a function of $\mu(t-\delta t)$, estimated from the O'Neill data. The second order regression relation of equation (14) is drawn, with neighbouring curves at $\pm$ one standard error of estimate.

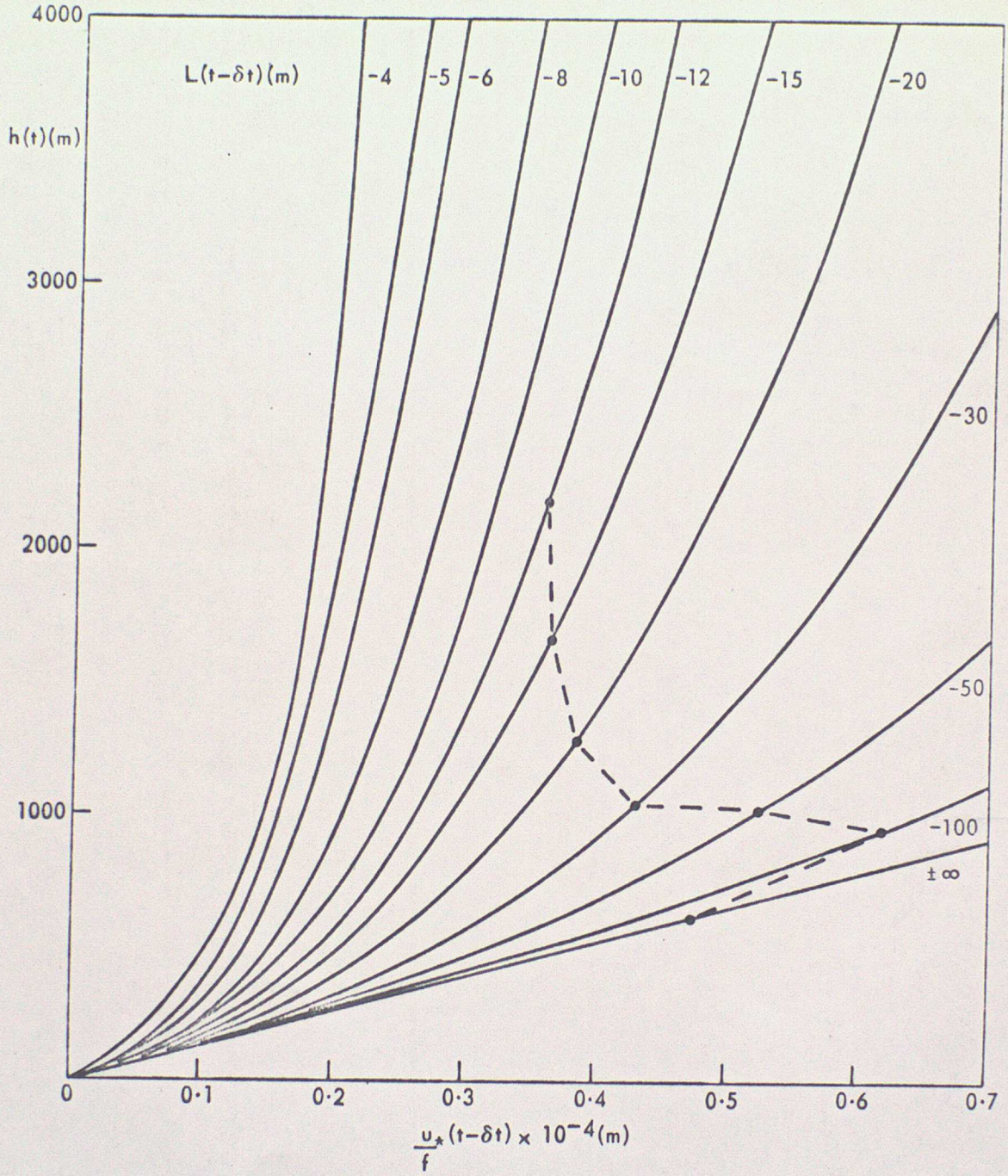

Figure 2. h(t)(m) as a function of $\frac{u_*}{f}(t-\delta t) \times 10^{-4}(m)$ and L(t-δt) (m), based on equation (15). The broken line indicates the order of h(t) (m) for typical values of (u_*/f, L) observed at O'Neill and illustrated in Figure 3.

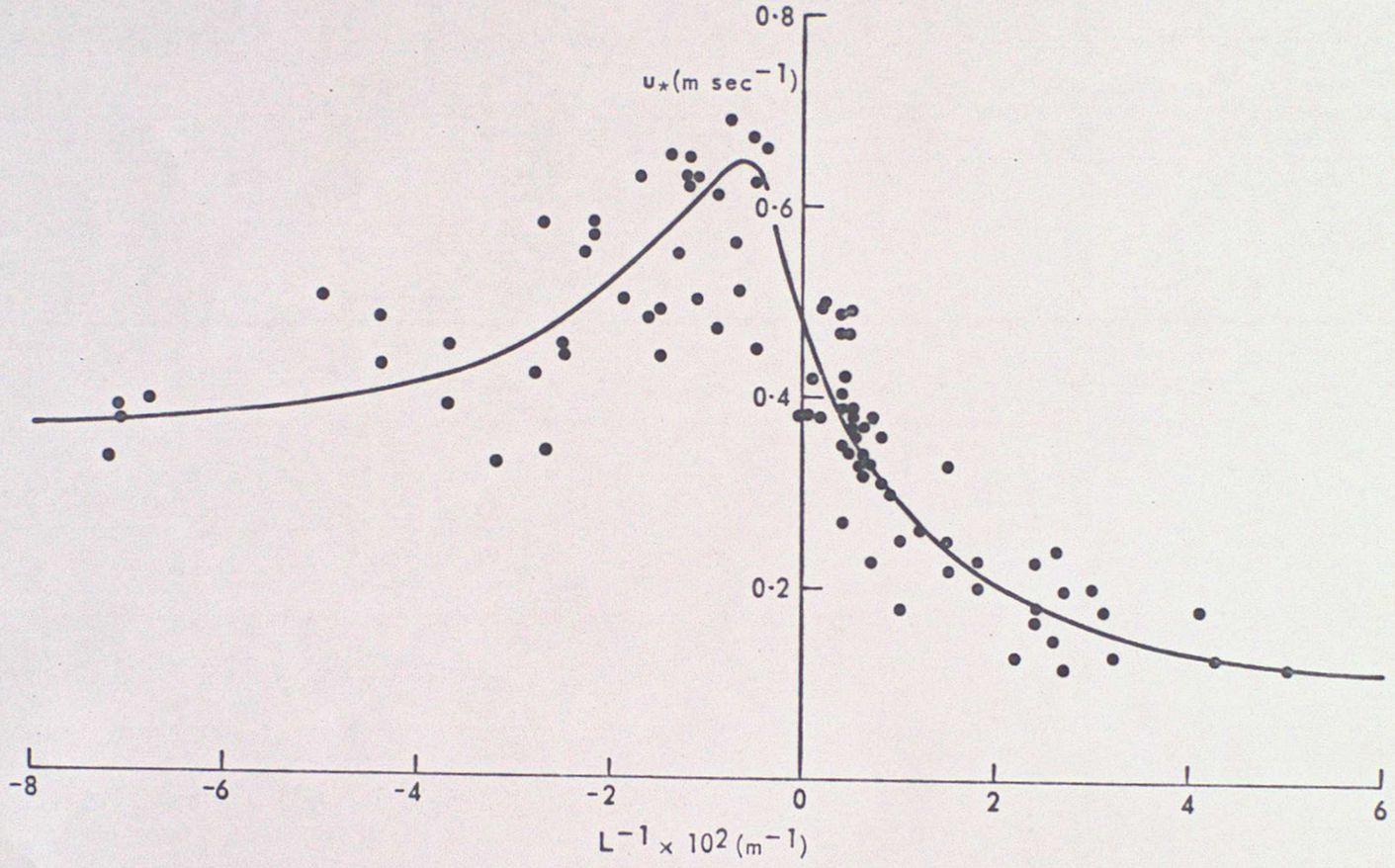

Figure 3. $u_*(m\ sec^{-1})$ as a function of $L^{-1} \times 10^2\ (m^{-1})$ observed at O'Neill. The curve is an eye fit.

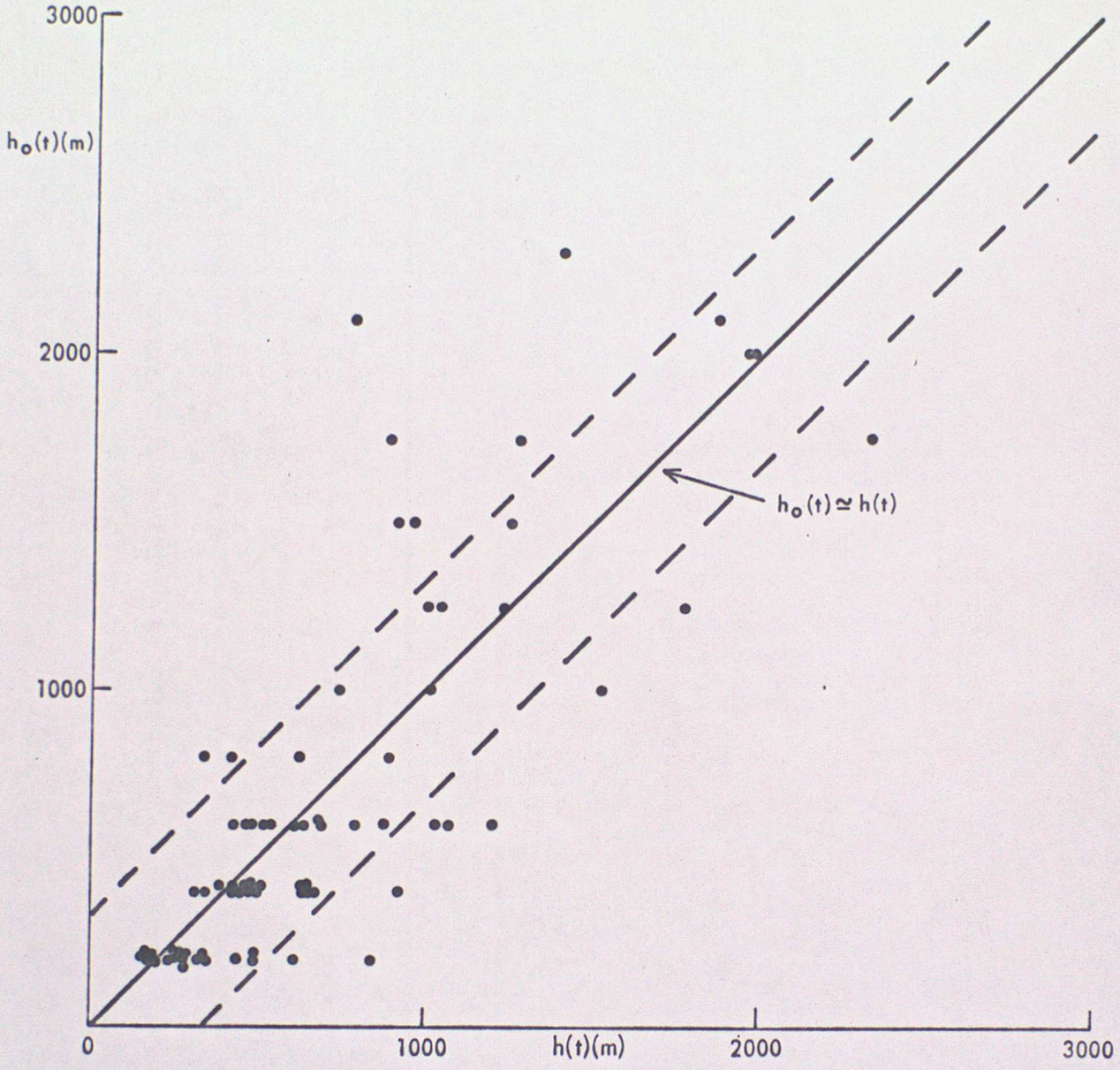

Figure 4. The observed boundary layer thickness $h_o(t)$ at O'Neill as a function of the theoretical estimate of the thickness $h(t)$ derived from equation (15). The straight line is the linear regression line, $h_o(t) \simeq h(t)$, with neighbouring lines at $\pm$ one standard error of estimate.

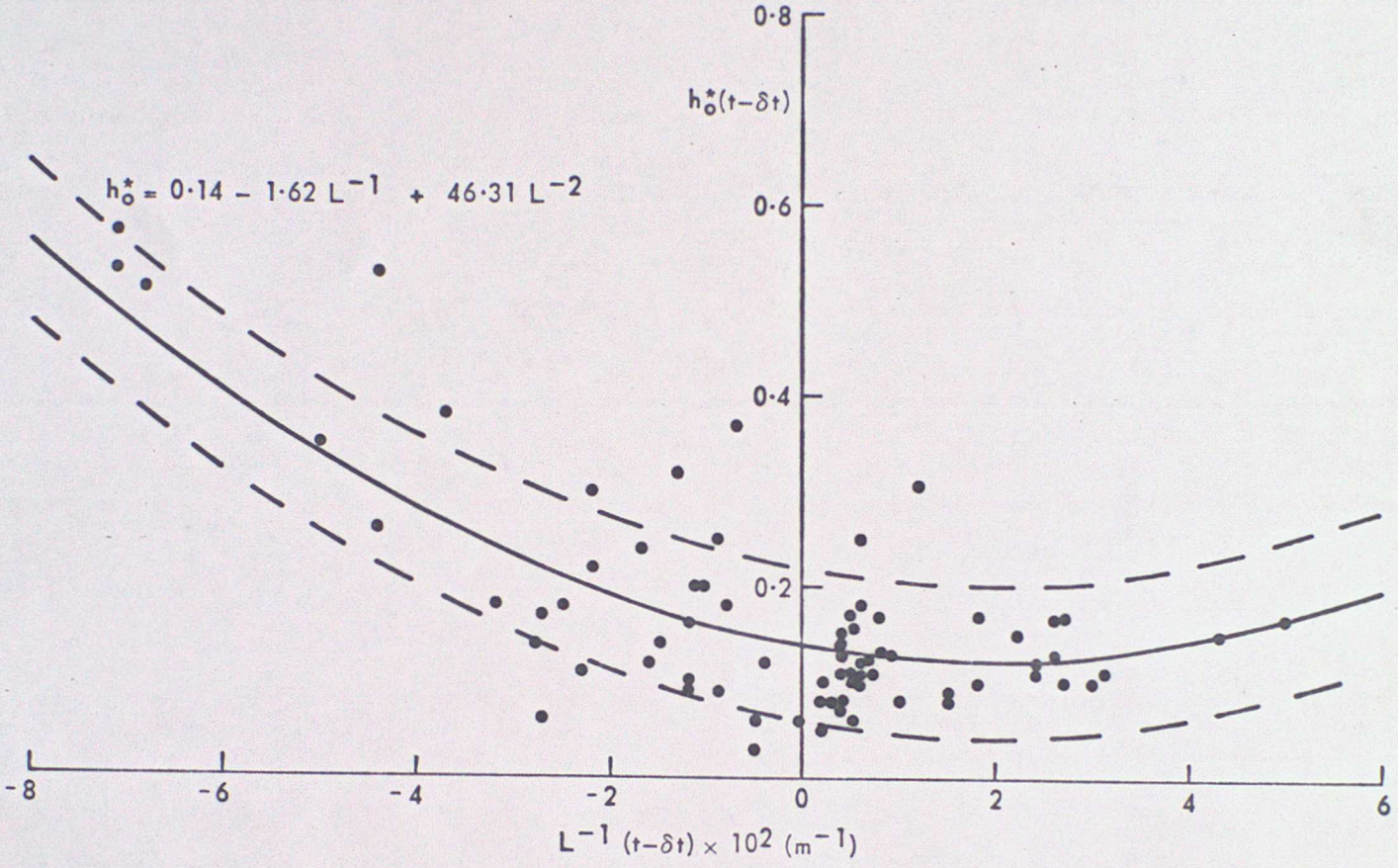

Figure 5. $h_o^*(t-\delta t)$ as a function of $L^{-1} \times 10^2 (m^{-1})$, estimated from the O'Neill data. The second order regression relation of equation (20) is drawn, with neighbouring curves at $\pm$ one standard error of estimate.

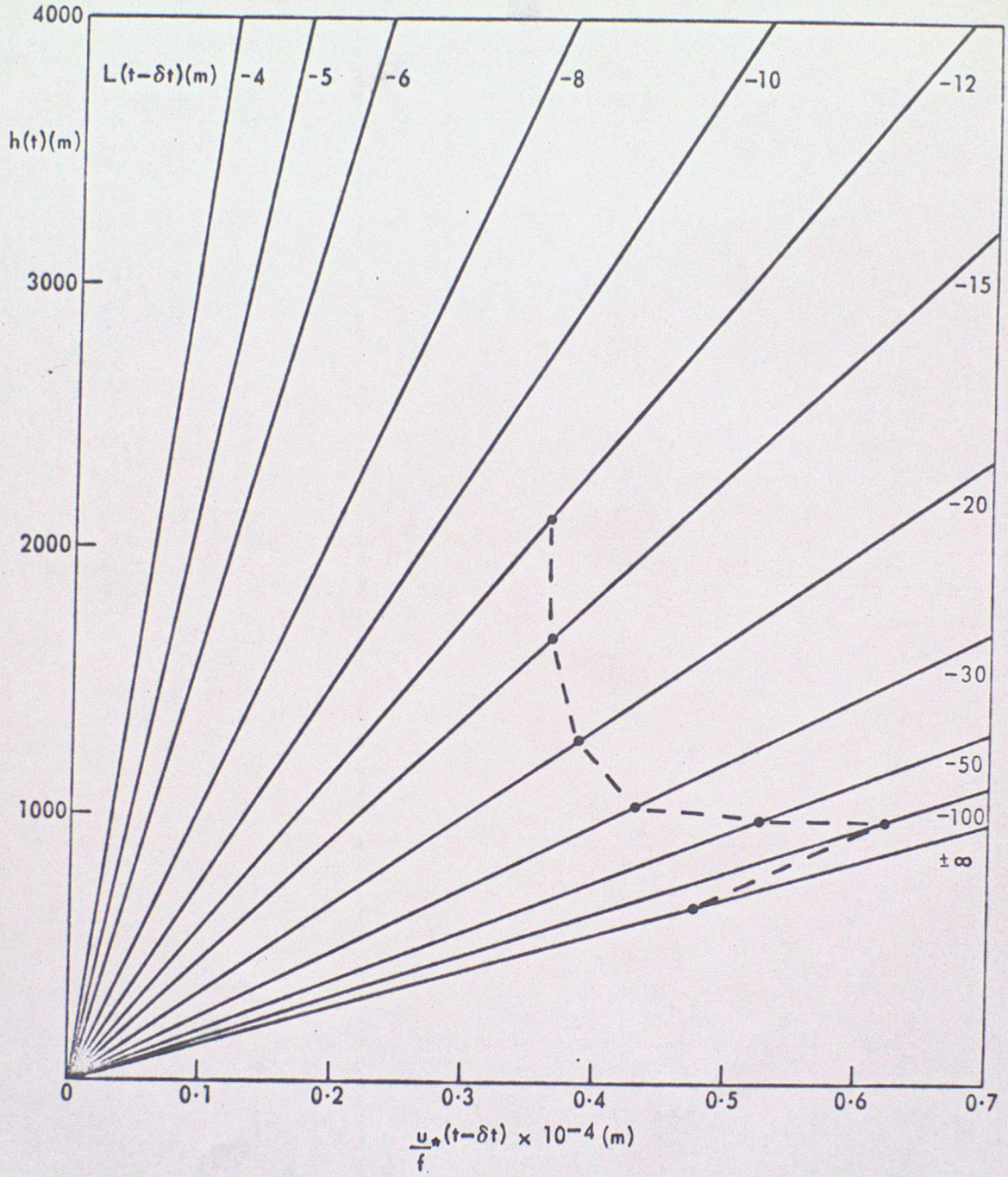

Figure 6. h(t) (m) as a function of $\frac{u_*}{f}(t-\delta t) \times 10^{-4}$(m) and L(t-δt) (m), based on equation (21). The broken line indicates the order of h(t) (m) for typical values of ($u_*/_f$, L) observed at O'Neill and illustrated in Figure 3.

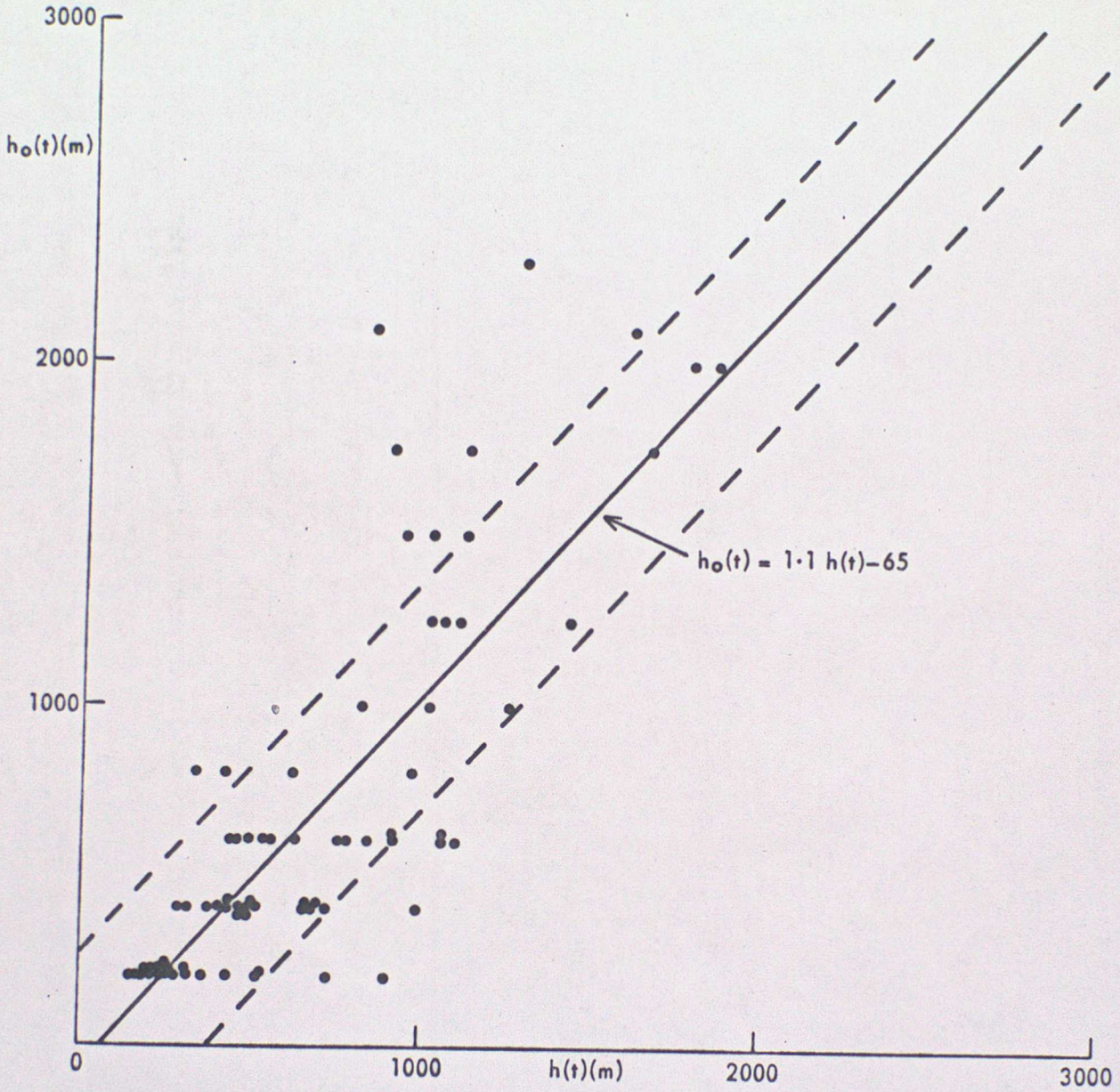

Figure 7. The observed boundary layer thickness $h_o(t)$ at O'Neill as a function of the theoretical estimate of the thickness $h(t)$ derived from equation (21). The straight line is the linear regression line, $h_o(t) = 1.1h(t)-65$, with neighbouring lines at $\pm$ one standard error of estimate.

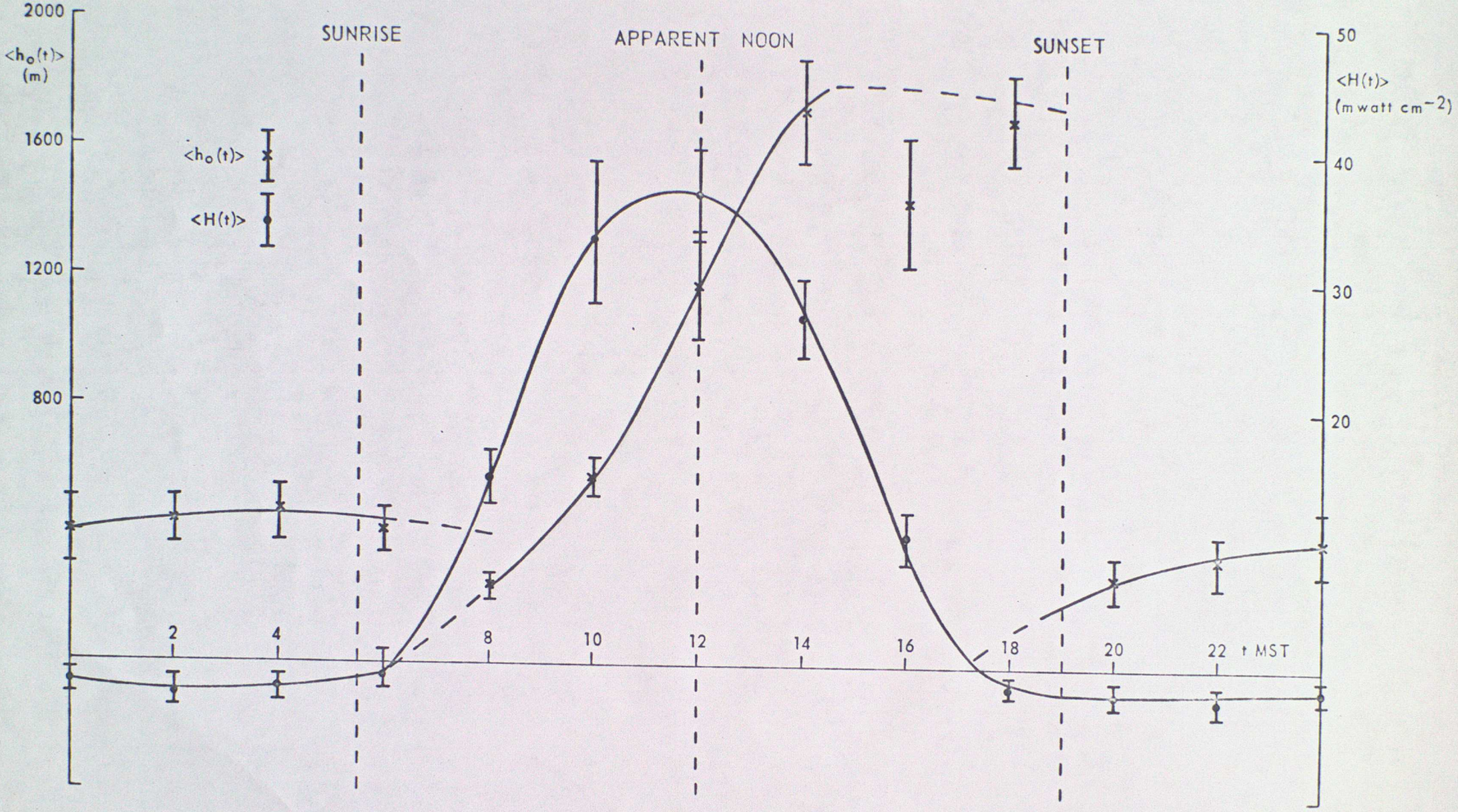

Figure 8. The mean boundary layer thickness, $\langle h_o(t) \rangle$, and sensible heat flux at the surface, $\langle H(t) \rangle$, deduced for the O'Neill data and plotted with standard errors as functions of time of day, t.

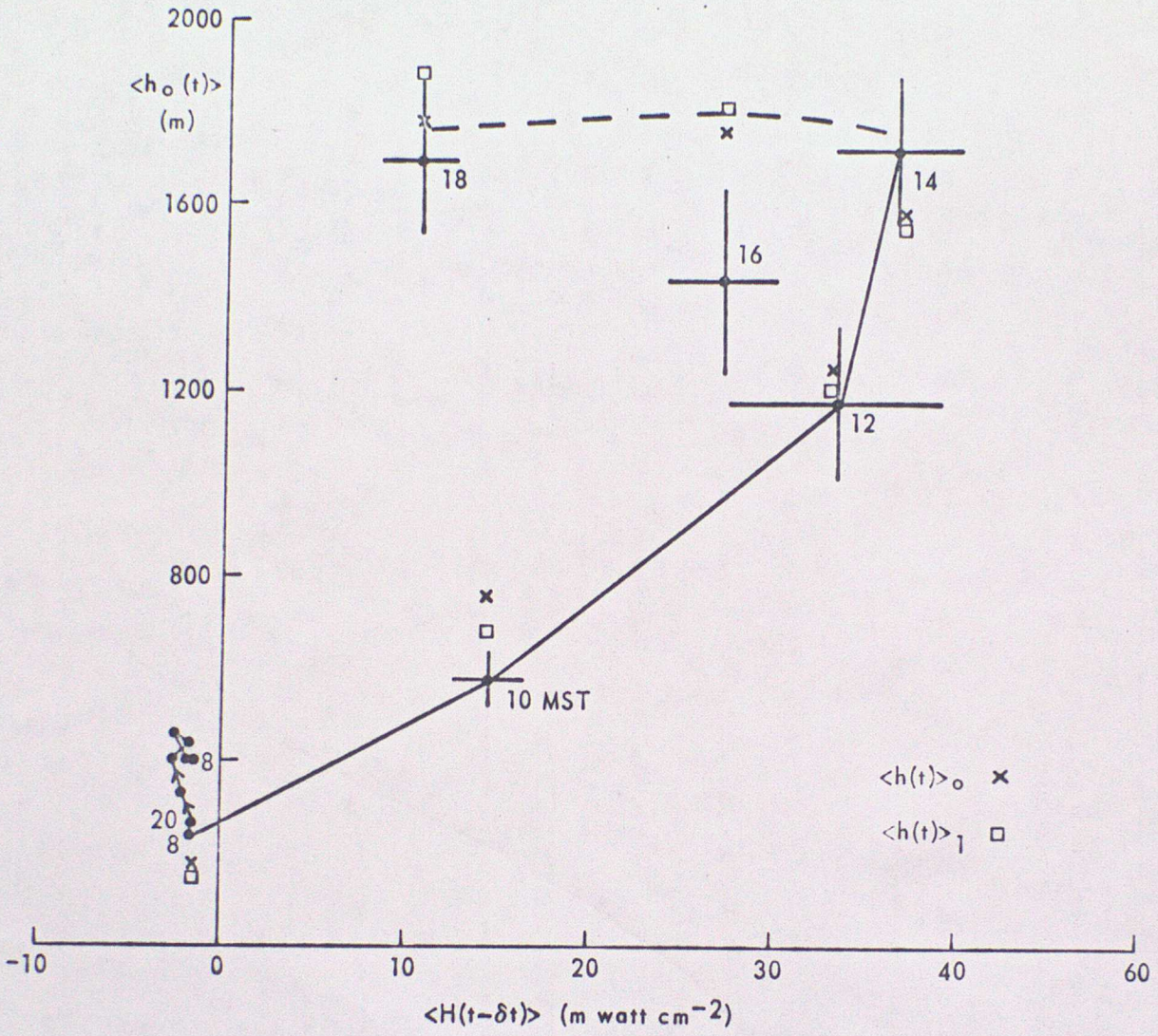

Figure 9. The mean observed boundary layer thickness $\langle h_o(t)\rangle$ at O'Neill as a function of the mean sensible heat flux $\langle H(t-\delta t)\rangle$ measured at an earlier period. The error bars on the points are the standard errors of the sample means, time t MST is given beside the points and δt is of order 2 hours. The curves indicate the daytime (0800 -1800 MST) and the night-time (2000-0800 MST) changes in the depth of the boundary layer. Also indicated are the estimated thicknesses $\langle h(t)\rangle_o$ and $\langle h(t)\rangle_1$, derived from equations (25) and (27) respectively.

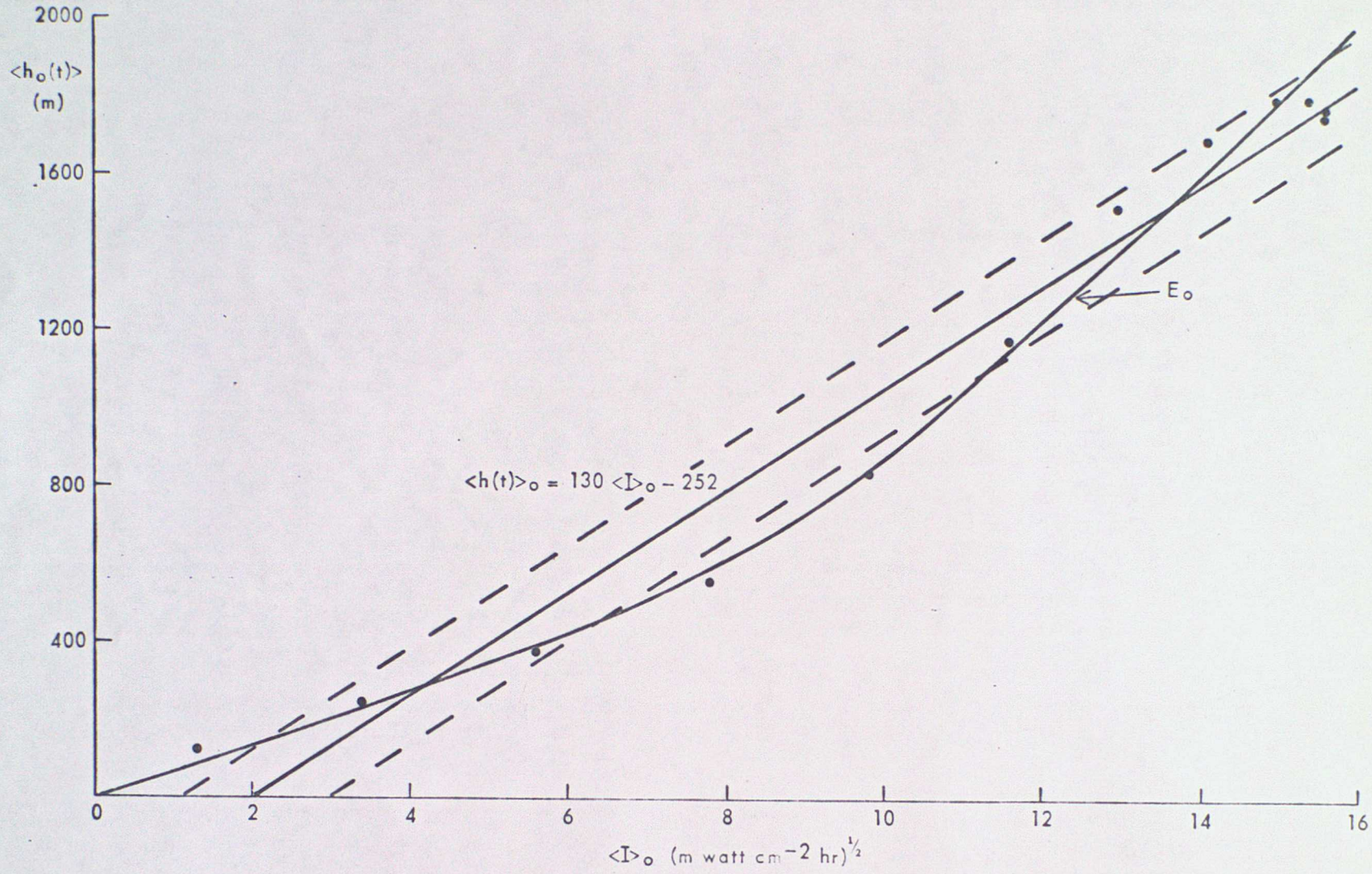

Figure 10. $\langle h_o(t) \rangle$ (m) as a function of $\langle I \rangle_o$ (m watt cm^{-2} hr)$^{\frac{1}{2}}$, estimated from the O'Neill data. The straight line is the linear regression line of equation (25) with neighbouring lines at $\pm$ one standard error of estimate, and the function, E_o, is a non-linear eye-fit curve.

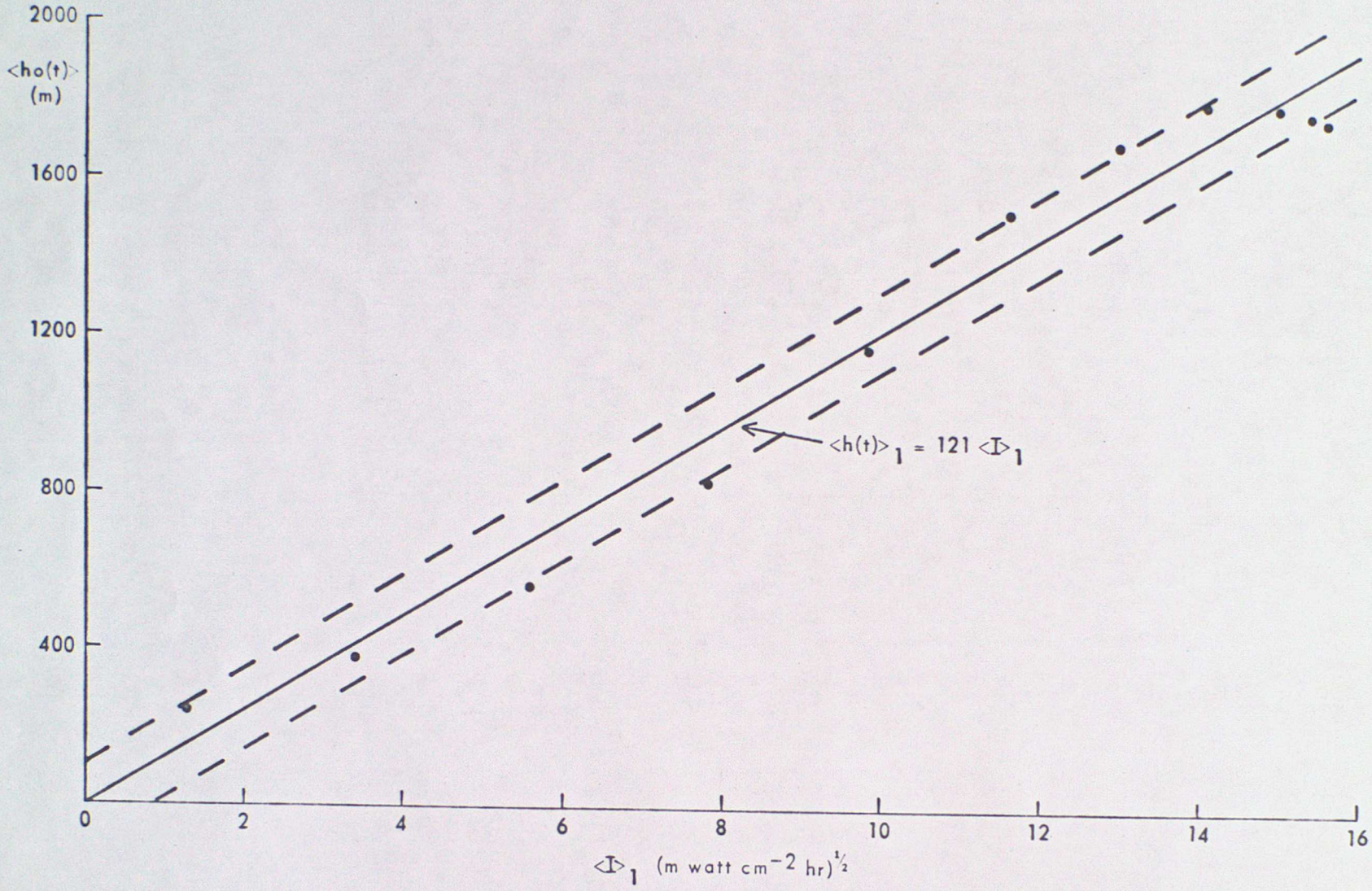

Figure 11. $\langle h_o(t) \rangle$ (m) as a function of $\langle I \rangle_1$, (m watt cm^{-2} hr)$^{\frac{1}{2}}$, estimated from the O'Neill data. The straight line is the linear regression line of equation (27) with neighbouring lines at $\pm$ one standard error of estimate.

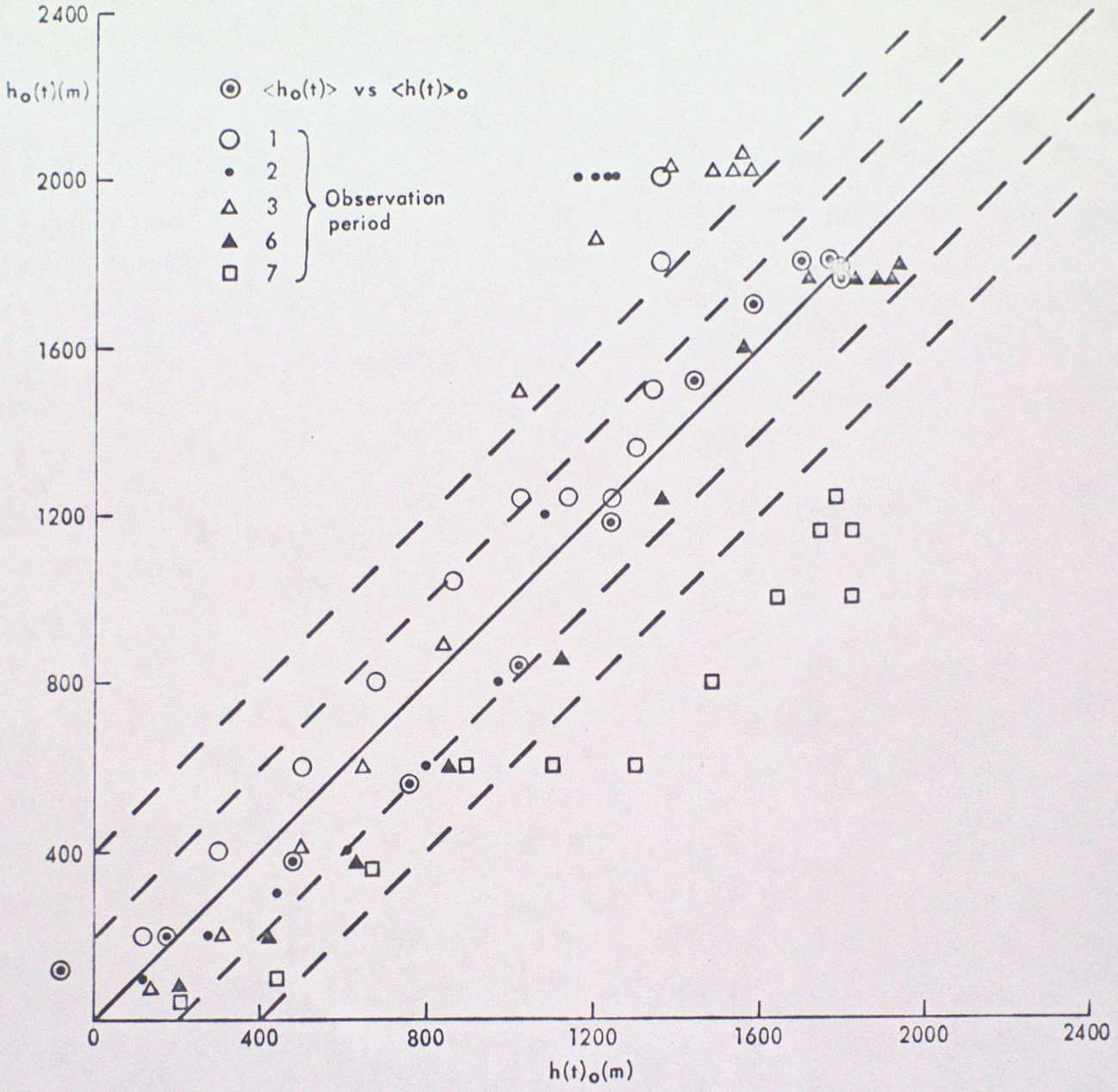

Figure 12. The observed boundary layer thickness $h_o(t)$ at O'Neill as a function of the theoretical estimate of the thickness $h(t)_o$ derived from equation (31). Lines are drawn at $h_o(t) = h(t)_o$; $h(t)_o \pm \frac{1}{2}$ standard error : $h(t)_o \pm$ one standard error.

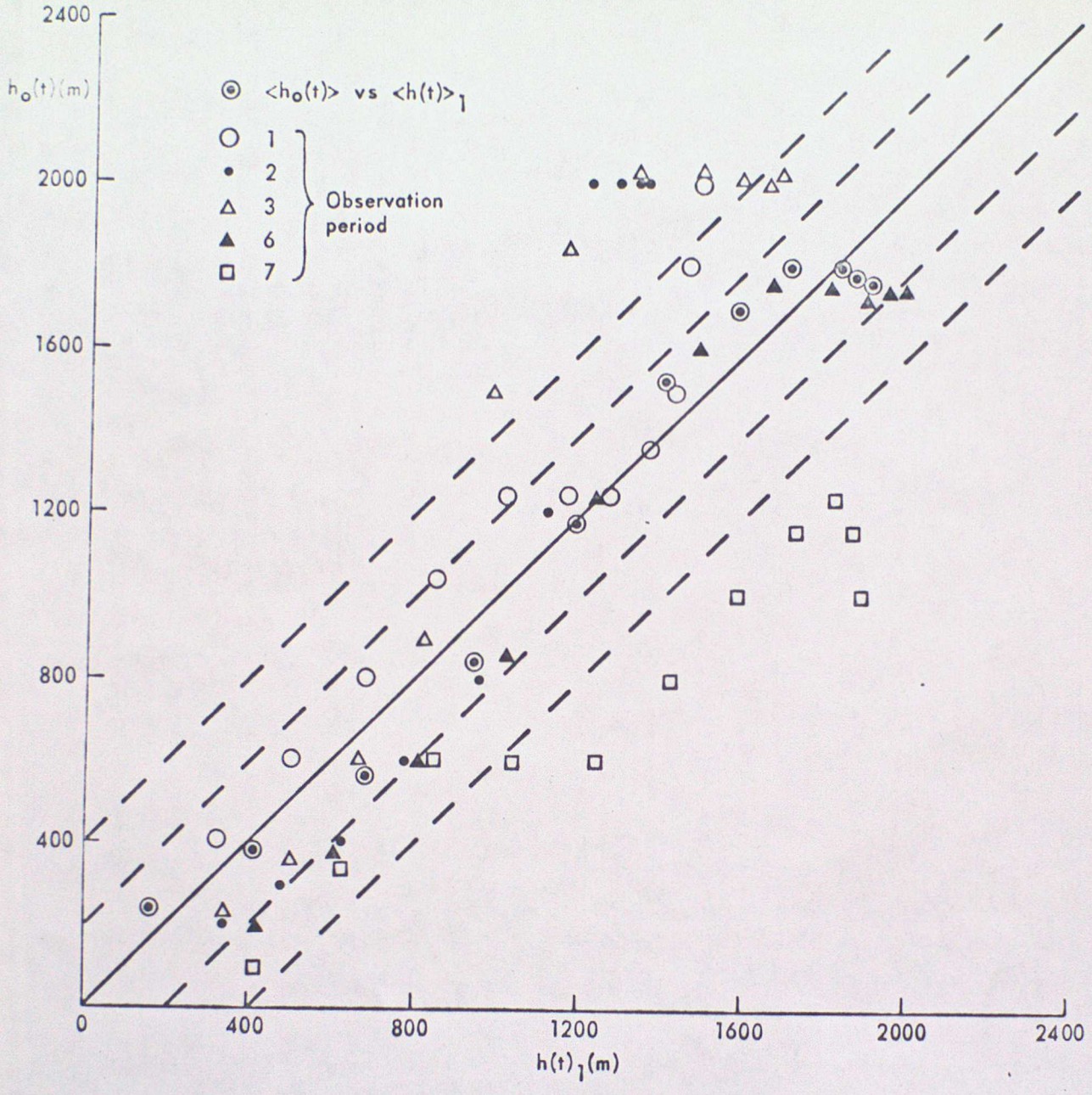

Figure 13. The observed boundary layer thickness $h_o(t)$ at O'Neill as a function of the theoretical estimate of the thickness $h(t)_1$. Lines are drawn at $h_o(t) = h(t)_1$; $h(t)_1 \pm \frac{1}{2}$ standard error ; $h(t)_1 \pm$ one standard error.